Chapter 2

Theory

2.1 Optimal control of quantum systems over finite time interval

In this section we present an analytical theory for optimal control of time-averaged quantities in quantum systems with relaxation.

In the first subsection a general variational formulation for the optimal control problem is given. The presented theory allows to describe optimal control of a quantum system over a finite [0,T] time interval. Optimal control of the system at a given time T is only a special case of our general theory. We also introduce a new type of constraint on the control field which limits the minimal width of the envelope of the resulting field. This constraint naturally arises if one tries to find the optimal pulses with experimentally achievable modulation of the control field.

In the second subsection we derive explicit ordinary differential equations for the optimal control fields using a certain functional form of the solution of the Liouville equation.

In the third subsection we derive an approximate analytical solution of the Liouville equation for the case of a two level system. We also analyze conditions under which the obtained solution is valid.

In the fourth subsection we present the analytical solution for the optimal control field for some simple problems. This is also a new result.

2.1.1 The Lagrangian formalism

Using the Lagrangian formalism for the control problem, it was shown [7, 8] how to construct optimal external fields to drive a certain physical quantity like the population of a given quantum state to reach a desired value at a given time. However, following the above cited procedures it is very difficult to obtain any analytical solution even for the simplest control problems.

In this section we develop a new theory that permits to obtain solutions of analytical form in some simple cases. The obtained solutions represent *global extrema* of the control problems. In order to solve the problem analytically we focus on the case of monochromatic control fields only. This means that we fix the carrier frequency and search for the optimal envelope of the field. Thus, we do not consider any frequency modulation in our theory. For simplicity we consider in this work only the case of one-photon resonance, however, our theory can be also applied when the multiphoton resonance takes place in the system [70].

Our method consists of two steps:

(1) Under certain conditions we derive an approximate analytical solution for the density matrix of the system that satisfies the quantum Liouville equation. This solution has a simple functional dependence on the control field.

(2) With the help of this solution we derive *an explicit ordinary differential equation* for the optimal control field.

Note, that one can guess the form of such equations from general physical arguments. Since memory effects are expected to be important, one should search for a differential equation containing both the pulse area θ [56] and its time derivatives $\dot{\theta}$, with θ defined as

$$\theta(t) = \mu \int_{t_0}^{t} dt' V(t'), \tag{2.1}$$

where $V(t)$ is the external field envelope, and μ being the dipole matrix element of the system. Therefore, for the case of optimal control of dynamical quantities at a given time t_0, the differential equation satisfied by $\theta(t)$ must be of at least second order to fulfill the initial conditions $\theta(t_0)$ and $\dot{\theta}(t_0) \equiv V(t_0)$. In the same way, the control of time averaged quantities over a finite time interval $[t_0, t_0 + T]$ with boundary conditions requires a differential equation of at least forth order for $\theta(t)$ due to the boundary conditions for $\theta(t)$ and $\dot{\theta}(t)$ at t_0 and $t_0 + T$. It will be shown below, that for certain quantum systems with relaxation a forth order differential equation for the control fields arises naturally using variational approach as an Euler-Lagrange (EL) equation.

Let us consider a quantum-mechanical system which is in contact with environment and interacting with an external field $E(t) = V(t)\cos(\omega t)$. Here $V(t)$ is a pulse shape and ω is a carrier frequency. The evolution of such system obeys the quantum Liouville equation for the density matrix $\rho(t)$ with dissipative terms. The control of a time averaged dynamical quantity requires the search for the optimal shape $V(t)$ of the external field.

Thus, in order to obtain the optimal shape $V(t)$ during a finite control time interval $[0, T]$ we propose the following Lagrangian (that is different

from the Lagrangian, proposed, for example, in [2] by Rabitz and coworkers)

$$L = \int_0^T \Theta(t)\Big(\frac{\partial}{\partial t} + i\hat{\mathcal{Z}}(t)\Big)\rho(t)dt + \beta\int_0^T \mathcal{L}_1 dt. \qquad (2.2)$$

β is a Lagrange multiplier and $\Theta(t)$ is a Lagrange multiplier density. Note, that throughout the section atomic units $\hbar$=m=e=1 are used.

The first term in Eq. (2.2) ensures that the density matrix satisfies the quantum Liouville equation with the corresponding Liouville operator $\hat{\mathcal{Z}}(t)$:

$$i\frac{\partial\rho}{\partial t} = \hat{\mathcal{Z}}(t)\rho(t). \qquad (2.3)$$

We assume that $\rho(t=0) = \rho_0$ is a density matrix corresponding to the initial conditions.

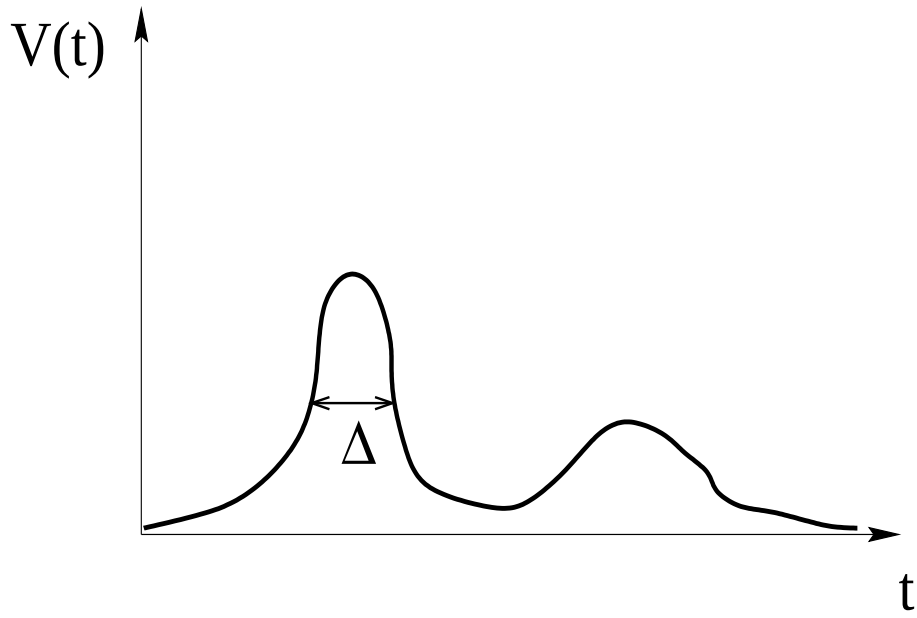

Figure 2.1: Constraint on the minimal width Δ of the envelope $V(t)$ of the optimal pulse (see Eq. [2.7]).

The second term in Eq. (2.2) explicitly includes the description of the optimal control. The functional density $\mathcal{L}_1$ is given by

$$\mathcal{L}_1(\rho(t), V(t), \frac{dV(t)}{dt}) = \mathcal{L}_{ob}(\rho(t)) + \lambda V^2(t) + \lambda_1\left(\frac{dV(t)}{dt}\right)^2, \qquad (2.4)$$

where λ and λ_1 are Lagrange multipliers. $\mathcal{L}_{ob}(\rho(t))$ refers to a physical quantity to be maximized during the control time interval. The control at a given time T can be obtained as a special case, as:

$$\int_0^T \mathcal{L}_{ob}(\rho(t))\delta(t-T)dt = \mathcal{L}_{ob}(\rho(T)), \tag{2.5}$$

where $\delta()$ is the Dirac delta function. The second term in Eq. (2.4) represents a constraint on the total energy E_0 of the control field

$$2\int_0^T E^2(t)dt \approx \int_0^T V^2(t)dt = \int_0^T \frac{\dot{\theta}^2(t)}{\mu^2}dt = E_0. \tag{2.6}$$

The third term in Eq. (2.4) represents a further constraint on the properties of the pulse envelope. The requirement

$$\int_0^T \left(\frac{dV(t)}{dt}\right)^2 dt = \int_0^T \frac{\ddot{\theta}^2(t)}{\mu^2}dt \leq R, \tag{2.7}$$

where R is a positive constant, bounds the time derivative of the pulse envelope $\frac{dV(t)}{dt}$ and therefore excludes infinitely narrow or abrupt step-like solutions, which cannot be achieved experimentally. Let Δ be a minimal experimentally achievable duration of the pulse, then $\Delta^{-1} \propto R$ (see Fig. [2.1]).

The above formulated control problem is highly complicated due to nonlinearity in the functional $\mathcal{L}_{ob}(\rho(t))$ and time dependence of the operator $\hat{\mathcal{Z}}(t)$ in the Liouville equation Eq. [2.3] that leads to a nontrivial dependence of the density matrix $\rho(t)$ on the field shape $V(t)$. However, we shall show that under certain conditions it is possible to obtain an analytical solution for the field envelope $V(t)$.

2.1.2 Derivation of the differential equation for the optimal control field

The formal solution of the Liouville equation Eq. [2.3] can be written in the time-ordered form:

$$\rho(t) = \hat{T}\exp\left(-\frac{i}{\hbar}\int_0^t \hat{\mathcal{Z}}(t)dt\right)\rho_0, \tag{2.8}$$

where $\hat{T}$ is the time ordering operator.

Let us assume that one can apply the Rotating Wave Approximation that eliminates fast oscillating terms like $\exp(i\omega t)$ and $\exp(-i\omega t)$ in the operator $\hat{\mathcal{Z}}(t)$, so in new variables the evolutionary operator $\hat{\tilde{\mathcal{Z}}}(V(t))$ depends only on the field envelope $V(t)$. Using the adiabatic approximation (see Appendix A), one can neglect the time ordering in Eq. [2.8]. Under this approximation the density matrix $\rho(t)$ depends only on the pulse area $\theta(t)$ and time t (see Appendix B), then we obtain an explicit expression for

the functional $\mathcal{L}_1 = \mathcal{L}_1(\theta, \dot{\theta}, \ddot{\theta}, t)$. The corresponding extremum condition $\delta\mathcal{L}_1 = 0$ yields the high-order Euler-Lagrange equation

$$-\frac{d^2}{dt^2}\frac{\partial \mathcal{L}_1}{\partial \ddot{\theta}} + \frac{d}{dt}\frac{\partial \mathcal{L}_1}{\partial \dot{\theta}} - \frac{\partial \mathcal{L}_1}{\partial \theta} = 0, \tag{2.9}$$

or, using Eq.(2.4)

$$-\lambda_1 \frac{d^4\theta}{dt^4} + \lambda \frac{d^2\theta}{dt^2} - \frac{\mu^2}{2}\frac{\partial \mathcal{L}_{ob}(\rho)}{\partial \theta} = 0. \tag{2.10}$$

In order to solve Eq. [2.10] one can assume natural boundary conditions $\theta(0) = \dot{\theta}(0) = \dot{\theta}(T) = 0$, $\theta(T) = \theta_T$, which also ensure that the control field is zero at the beginning and at the end of the control interval: $V(0) = V(T) = 0$. The choice of the constant θ_T depends on the control problem. In general, the constants θ_T, R and E_0 can be also object of the optimization. Note, that Eq. [2.10] is highly nonlinear with respect to the pulse area $\theta(t)$ and usually can be solved only numerically. However, using Eq. [2.10] we shall obtain some *analytical* solutions for simple control problems, which were not known before.

Eq. [2.10] is the kernel of the presented theory and provides an explicit ordinary differential equation for the pulse area $\theta(t)$. Note, that this equation is only applicable if one is able to determine an approximate explicit expression for the density matrix $\rho \approx \rho(\theta(t), t)$. In order to show

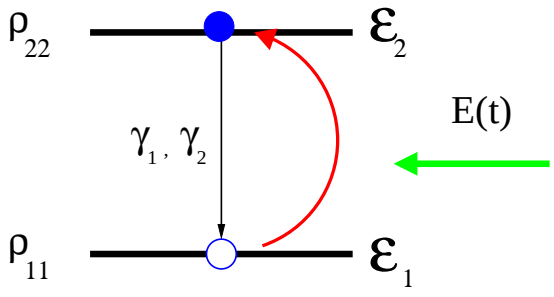

Figure 2.2: A two level system with energy levels ϵ_1,ϵ_2 interacting with resonant external field $E(t)$ and characterized by relaxation and dephasing constants γ_1,γ_2 (see text). The occupations of the levels are described by diagonal density matrix elements ρ_{11} and ρ_{22}.

that Eq. [2.10] can describe optimal control in real physical situations, we apply our theory to a two level quantum system with relaxation (see Fig. [2.2]).

2.1.3 An approximate analytical solution for the case of a two level system

In order to illustrate our approach let us consider control of a two level system. We represent the system Hamiltonian $\hat{H}_0$ plus interaction with external field $E(t) = V(t)\cos(\omega t)$ in the form:

$$\hat{H} = \hat{H}_0 + \hat{H}_{int} = \begin{pmatrix} \epsilon_1 & 0 \\ 0 & \epsilon_2 \end{pmatrix} + \begin{pmatrix} 0 & -\mu_{12}E(t) \\ -\mu_{21}E^*(t) & 0 \end{pmatrix} \tag{2.11}$$

where ϵ_1 and ϵ_2 are energy levels, $\mu_{12} = \mu_{21}^*$ is a dipole matrix element, and the sign * denotes complex conjugation. Without loosing the generality one can set $\mu_{21} = \mu_{12} = 1$. This means that we measure the field amplitude in energy units. Evolution of the system is described by the Liouville equation for the density matrix $\rho(t)$ [72]:

$$\begin{aligned} i\frac{\partial \rho_{11}}{\partial t} &= E^*(t)\rho_{21} - E(t)\rho_{12} + i\gamma_1\rho_{22}, \\ i\frac{\partial \rho_{22}}{\partial t} &= E(t)\rho_{12} - E^*(t)\rho_{21} - i\gamma_1\rho_{22}, \\ i\frac{\partial \rho_{12}}{\partial t} &= \omega_0\rho_{12} + E(t)(\rho_{22} - \rho_{11}) - i\gamma_2\rho_{12}, \\ \rho_{21} &= \rho_{12}^*, \end{aligned} \tag{2.12}$$

where $\omega_0 = \epsilon_2 - \epsilon_1$ and γ_1 and γ_2 are relaxation and dephasing constants, respectively. Eqs. [2.12] are used for the description of different effects, like for instance, the response of donor impurities in semiconductors to terahertz radiation [12], or the excitation of surface- into image charge states at noble metal surfaces [53]. Let us assume that the carrier frequency of the control field ω is chosen to be the resonant frequency $\omega = \omega_0$. Using the Rotating Wave Approximation one derives the following equations:

$$\begin{aligned} i\frac{\partial \rho_{\ell\ell}}{\partial t} &= (-1)^\ell(V(t)(\tilde{\rho}_{21} - \tilde{\rho}_{12}) - i\gamma_1\rho_{22}), \\ i\frac{\partial \tilde{\rho}_{12}}{\partial t} &= V(t)(\rho_{22} - \rho_{11}) - i\gamma_2\tilde{\rho}_{12}, \end{aligned} \tag{2.13}$$

where $\ell = 1, 2$ and

$$\begin{aligned} \tilde{\rho}_{12} &= \rho_{12}\exp(i\omega t), \\ \tilde{\rho}_{21} &= \rho_{21}\exp(-i\omega t). \end{aligned} \tag{2.14}$$

Note, that $\rho_{11} + \rho_{22} = 1$ and $\tilde{\rho}_{21} = \tilde{\rho}_{12}^*$. We set the initial conditions as $\rho_{11} = 1, \rho_{22} = \tilde{\rho}_{12} = \tilde{\rho}_{21} = 0$.

Eqs. [2.13] have the form $i\partial\rho(t)/\partial t = \hat{\tilde{\mathcal{Z}}}(t)\rho(t)$ and are difficult to integrate, since the operator $\hat{\tilde{\mathcal{Z}}}(t)$ explicitly depends on time, or in other words, the commutators $[\hat{\tilde{\mathcal{Z}}}(t), \hat{\tilde{\mathcal{Z}}}(t')] \neq 0, t \neq t'$. However, the commutators $[\hat{\mathcal{Z}}(t), \hat{\mathcal{Z}}(t')]$ become arbitrarily small under the condition (see Appendix B)

$$\left| \frac{\gamma_\ell T^2}{V(t)} \left(\frac{\partial V(t)}{\partial t}\bigg|_{t'} \right) \right| \ll 1, \tag{2.15}$$

with $\ell = 1, 2$, and we obtain an approximate solution for the density matrix $\rho(t)$ (see Appendix B). For the occupation of the excited level $\rho_{22}(t)$ this solution reads:

$$\rho_{22}(t) = 2\theta^2(t)F^{-1}\Big(1 - \cosh(H)\exp(-(\gamma_1+\gamma_2)t/2) \\ +(\gamma_1+\gamma_2)t\ \sinh(H)\exp(-(\gamma_1+\gamma_2)t/2)H^{-1}\Big), \tag{2.16}$$

where

$$H = \sqrt{((\gamma_1-\gamma_2)^2t^2 - 16\theta^2(t))}/2,$$

and

$$F = \gamma_1\gamma_2t^2 + 4\theta^2(t).$$

Note, that this approximate solution becomes exact when $\gamma_1 = \gamma_2 = 0$ or for a constant amplitude of the control field $V(t) = V_0$, that is reflected by Eq. [2.15]. The expression of Eq. [2.16] has the form $\rho = \rho(\theta(t), t)$ and therefore Eq. [2.10] is applicable.

In order to determine the control problem let us construct the functional density

$$\mathcal{L}_{ob}(\rho) = \frac{1}{T}\rho_{22}(t), \tag{2.17}$$

so that an average occupation of the upper level $n_2 = \frac{1}{T}\int_0^T \rho_{22}(t)dt$ is the quantity to be maximized. Note, that n_2 is proportional to the observed photo-charge in the terahertz experiments on semiconductors [12]. The resonant tunneling photo-charge through an array of coupled quantum dots is also proportional to such a value [54].

2.1.4 The analytical solution for the optimal control field with a simplified Lagrangian

In order to obtain an analytical solution for the optimal control field, we analyze the problem in certain limiting cases. For instance, if $\gamma_{1,2}T \ll 1$ one can neglect relaxation and dephasing effects within the control interval and Eq. (2.16) becomes $\rho_{22}(t) = \sin^2(\theta(t))$. In order to make the problem

analytically solvable, we reduce the order of the Euler-Lagrange equation Eq. [2.10]. For that purpose we exclude the constraint on the derivative of the field envelop (see Eq. [2.7]). Thus, the Lagrangian density $\mathcal{L}_1$ for optimal control becomes

$$\mathcal{L}_1 = \rho_{22}(t)/T + \lambda\dot{\theta}^2(t)/\mu^2, \tag{2.18}$$

while the corresponding Euler-Lagrange equation is given by

$$2\lambda\ddot{\theta}(t) - \mu^2 \sin(2\theta(t))/T = 0. \tag{2.19}$$

The second order differential Eq. (2.19) requires two boundary conditions, for which we choose $\theta(0) = 0$ and $\theta(T) = \pi/2$ (which ensure the population inversion). Eq. [2.19] is similar to the equation for a mathematical pendulum and can be solved analytically (see Appendix D). The resulting field envelope $V(t)$ is given by the expression

$$V(t) = V(0)\, dn(\mu V(0)t, B), \tag{2.20}$$

where dn is the Jacobian elliptic function, and $B = -(\lambda T V^2(0))^{-1}$. Note that the control field is nonzero at the beginning $V(0) \neq 0$. Eq. [2.20] can be understood as a limiting case of the solution of the equation Eq. [2.10] with $\lambda_1 \to 0$ and $R \to \infty$. The corresponding optimal dynamics of $\rho_{22}(t)$ in these two cases is similar.

Using the condition given by Eq. [2.6] for the pulse energy E_0 we determine the Lagrange multiplier λ. In the limit $B \to 1$ that corresponds to the case of rapid excitation (all pulse energy is concentrated in the beginning of the control interval) the formula given by Eq. [2.20] can be significantly simplified to

$$V(t) = \frac{1}{\mu}\frac{\partial}{\partial t}\arccos[2\exp(\mu V(0)t)/(1+\exp(2\mu V(0)t))]. \tag{2.21}$$

Let us now consider the opposite control problem, namely the problem to **minimize** the integral over the occupation of the excited level $n_{inf} = \int_{-\infty}^{+\infty} \rho_{22}(t)dt$. We consider infinitely large control interval $t \in (-\infty, \infty)$ with natural boundary conditions $V(-\infty) = V(+\infty) = 0$ and $\theta(+\infty) = \pi$. Thus, the system remains in the ground state after the interaction with the control field. Integrating the corresponding Euler-Lagrange equation one can easily obtain that the optimal field in this case is described by a soliton solution (see Fig. [2.3]):

$$V(t) = (\sqrt{\lambda}\cosh((t)/\sqrt{\lambda/\mu^2})^{-1}. \tag{2.22}$$

Using the normalization condition for the pulse energy E_0 given by Eq. [2.6], we obtain that

$$\lambda = \Big(\frac{2}{\mu E_0}\Big)^2. \tag{2.23}$$

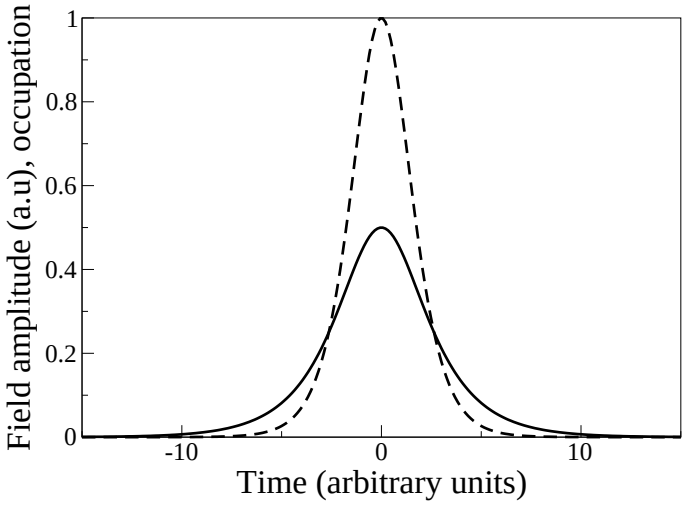

Figure 2.3: Solid line: the soliton solution for the optimal control field $V(t)$ which minimizes the value of n_{inf} (see text). Dashed line: corresponding dynamics of the occupation of the upper level $\rho_{22}(t)$.

This remarkable result means that the soliton Eq. [2.22] is not only one possible solution that propagates without losses (since we have no spatial variable one can treat the Eq. [2.19] as the sine-Gordon equation in the limit of the optically thin media), but it also minimizes the energy losses which are proportional to n_{inf} in the limit of the weak relaxation and dephasing. Using other asymptotic values of the pulse area $\theta(+\infty) = N\pi$, where N is an integer number $N = 2, 3, ...$, one can immediately reproduce $2\pi, 3\pi...$ soliton solutions.

2.1.5 Optimal control at a given time

Now we show that there is an essential difference between optimal control in order to maximize an objective at a given time T or to maximize the same objective over time interval $[0, T]$. For this purpose we consider instead of Eq. [2.18] the Lagrangian density:

$$\mathcal{L}_1 = \rho_{22}(T) + \lambda\dot{\theta}^2(t)/\mu^2, \tag{2.24}$$

that corresponds to a problem of maximization of the occupation of the upper level $\rho_{22}(T)$ at a given time T. In order to make a comparison with the solution given by Eq. [2.20] we set $\gamma_1 = \gamma_2 = 0$. Using the same procedure, as for derivation of Eq. [2.19], we obtain the corresponding Euler-Lagrange equation

$$2\lambda\ddot{\theta}(t) - \mu^2\delta(T-t)\sin(2\theta(t)) = 0. \tag{2.25}$$

The solution of Eq. (2.25) is a field with constant amplitude of the envelope

$$V(t) = \frac{\pi}{2T\mu}, \tag{2.26}$$

that reflects the fact that there is only one optimal pulse with energy $E_0 = \pi^2/(4T\mu^2)$ which drives the occupation ρ_{22} to 1 at given time T. This analytical result one can compare with the numerical solution for the similar problem obtained by Wusheng Zhu, Jair Botina, and Herschel Rabitz by using the iterative numerical technique [10].

From the comparison between solutions Eqs. [2.20] and [2.26] one can conclude, that the formulation of the optimal control over time interval is a nontrivial generalization of the optimal control theory, and permits to perform more detailed coherent control of quantum systems.

The Lagrangian density of the form of Eq. [2.18] or Eq. [2.24] always leads to a second order differential equation for the control field which can be easily integrated analytically, as long as the approximation $\rho \approx \rho(\theta(t), t)$ holds. However, the obtained optimal field $V(t)$ cannot satisfy boundary conditions $V(0) = V(T) = 0$. Otherwise one would obtain a trivial solution $V(t) \equiv 0$, which is not consistent with the condition on the pulse energy (see Eq. [2.6]). In order to impose conditions on $V(0)$ and $V(T)$ a Lagrangian leading to a forth order differential equation is necessary. Despite of the fact that the optimal control fields with the same energy will satisfy different boundary conditions, the corresponding dynamics of the optimally controlled system $\rho(t)$ will be quit similar in both cases.

2.1.6 Estimation of the absolute bound for the control due to relaxation and dephasing effects

As it was recently shown [7], the relaxation and dephasing processes in the systems creates obstacles for the optimal control. In order to estimate quantitatively, how relaxation and dephasing processes limit control of the time average of the occupation of upper level n_2, we analyze the occupation $\rho_{22}(t)$ (see Eq. [2.16]) in more detail. In the limit of a strong control field satisfying

$$\gamma_{1,2}t/\theta(t) \ll 1, \; t \in [0, T], \tag{2.27}$$

that means that excitation of the system prevails over relaxation processes, the Eq. [2.16] can be significantly simplified and one finds that the instantaneous occupation $\rho_{22}(t)$ lies always lie under the curve $\rho_{22}^{max}(t) = (1 + \exp(-(\gamma_1 + \gamma_2)t/2))/2$. This means that $\rho_{22}(t)$ exhibits an absolute upper bound. In order to illustrate this bound we plot in Fig. [2.4] the dynamics of the occupation $\rho_{22}(t)$ for 40 randomly generated control pulses applied to a two level system with relaxation and dephasing parameters $\gamma_1 T = 2\gamma_2 T = 1$ and setting $T = 1$. Therefore, due to dissipative pro-

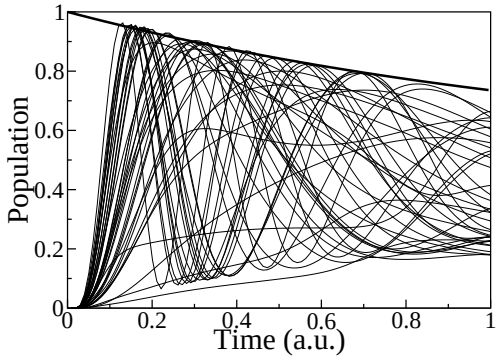

Figure 2.4: Dynamics of the occupation $\rho_{22}(t)$ for 40 randomly generated control pulses using $\gamma_1 T = 2\gamma_2 T = 1$ (thin solid lines). The thick solid line represents a bound for the possible values of $\rho_{22}^{max}(t) = (1 + \exp(-(\gamma_1 + \gamma_2)t/2))/2$.

cesses the following inequality holds for the controlled averaged value of ρ_{22}:

$$n_2 \leq \frac{1}{T}\int_0^T \rho_{22}^{max}(t)dt = 1/2 + \frac{(1 - \exp(-(\gamma_1 + \gamma_2)T/2)}{(\gamma_1 + \gamma_2)T}. \qquad (2.28)$$

Using this inequality one can estimate the maximal possible value of n_2 for given parameters of the problem γ_1, γ_2, T.

Using the expression Eq. [2.28], let us investigate two limiting cases. For a system with weak relaxation and dephasing ($\gamma_{1,2}T \ll 1$) the populations can be fully inverted and remain in this state during the control time interval so that $\rho_{22}(t) \simeq 1$, the maximum possible value of the controlled quantity is $n_2 = 1$. In the limit of strong relaxation and dephasing $\gamma_{1,2}T \simeq 1$ system is in the saturation regime, so that ground and excited levels are approximately equally occupied within control interval and $n_2 \simeq 0.5$.

It is not possible to overcome the limit given by Eq. [2.28] within the considered model. The optimal pulse that satisfies Eq. [2.10] provides the highest possible value of the objective for a given pulse energy. For example, in comparison with pulses having square amplitude or Gaussian pulses, the optimal fields, obtained in our calculations, lead to a value of n_2, that is up to 50% higher.

With Eq. [2.28] we can, for example, estimate the maximal possible lifetime for an excited (image) electron state at a Cu(111) surface which can be achieved by application of the control field with a proper pulse shaping. According to Hertel et al. [53], those states are characterized by $\gamma_1 = 5 \cdot 10^{13} s^{-1}$ and $\gamma_2 = \gamma_1/2$. Thus, our theory predicts in that case an effective decay constant $\gamma_{eff} \geq (\gamma_1 + \gamma_2)/2 = 3.75 \cdot 10^{13} s^{-1}$. By controlling the excitation of the surface states one can possibly achieve an enhancement of certain chemical reactions.

2.2 Calculation of the excitation spectrum of quantum systems using genetic algorithms

In this section we present a new method to calculate the excitation spectra of few-body quantum systems. Our theory is based on a variational formulation of the eigenvalue problem. Thus, we can treat it as an optimization problem. In order to perform an effective search for the optimum we use genetic algorithms (GA). This technique is orders of magnitude faster than, for instance, the random walk (Monte Carlo) method [58]. However, the direct application of the GA to quantum problems is not possible due to reasons which will be described below. Therefore, we formulate an extended method which we call Quantum Genetic Algorithm (QGA) and which can be applied to various quantum mechanical systems.

In the first subsection we give a short introduction to the evolutionary algorithms, which we use for almost all sections of the present work.

In the second subsection we outline the main principles of the QGA, which is the first formulation of the genetic algorithm for quantum problems.

2.2.1 Introduction to evolutionary algorithms

Genetic algorithms were formally introduced in the 1970s by John Holland at University of Michigan [78, 79]. Genetic algorithms are especially useful for treating strongly nonlinear physical systems with a complicated (multi-dimensional, etc.) configurational space and where a hint of the optimal state (for instance, the ground state) is very difficult. Rather than looking for the optimal state by performing small variations of a single trial function, a more effective strategy is used which includes in addition more drastic changes. These may consist of combining states which are taken from the pool of trial states. A possible improvement with respect to the optimal state is controlled by the decrease of the energy, for example, which is a kind of a fitness test. This strategy is reminiscent of the evolution in life. The set of trial states corresponds to a population, the drastic changes to the crossover between genomes of two members of the population, and the control function for survival and adaptation. Small changes consisting of local variations of a single trial solution are also included and correspond to mutations.

The genetic algorithm creates an initial population of solutions, and applies genetic operators such as mutation and crossover [80] to evolve the solutions in order to find the best one(s). Genetic algorithms belong to the class of stochastic search methods (other stochastic search methods include, for example, simulated annealing [59]). Whereas most stochastic

search methods operate on a single solution for the problem under consideration, genetic algorithms operate on a population of trial solutions.

Let us outline some basics of genetic algorithms. The three most important aspects of using genetic algorithms are:

1. definition of the objective (fitness) function,
2. definition and implementation of the genetic representation,
3. definition and implementation of the genetic operators.

The genetic algorithm is very simple, yet it performs well on many different types of problems. However, there are many ways to modify the basic algorithm, and many parameters can be varied. Basically, in the case of the correctly chosen objective function, representation of the solutions and genetic operators, any further variations of the genetic algorithm and its parameters will result in only minor improvements. Following the seminal work of Holland [78], the most common representation for the individual genomes in the genetic algorithm is a string of bits. The reason is that the definition of the genetic operators in this case is very simple.

Let us now discuss the main genetic operators: copy, crossover and mutation. The copy or reproduction operator simply transfers the information of a "parent" to an "offspring" of the next generation without any changes. Typically the crossover is defined by the consideration of two individuals (the "parents") in order to produce two new individuals (the "children"). The primary purpose of the crossover operator is to transfer genetic material from the previous generation to the subsequent generation. In a simple crossover operation, a random position in the string of

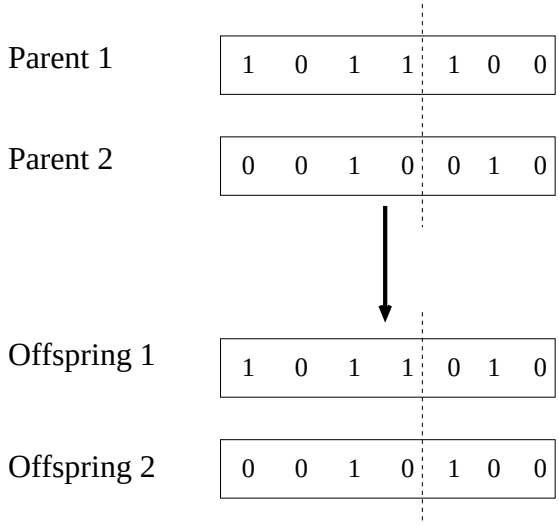

Figure 2.5: Illustration of the crossover operation between randomly chosen Parents 1 and 2 at a random position (marked by dashed line). The parents exchange their genetic material in order to generate two new offsprings.

bits is chosen at which each partner in a randomly chosen pair of "parents" is divided into two parts. Each parent vector then exchanges a subsection of itself with its partner (see Fig.[2.5]). The application of the crossover operation between identical "parents" leads to the same "children".

The mutation operator introduces a certain amount of randomness to the search. It helps the search to find solutions which the crossover operation alone cannot encounter. Usually the mutation operation applies the logical "NOT" (negation) operation to a single bit of a randomly chosen single "parent" at a random position.

Two of the most common implementations of the genetic algorithm are called "simple" and "steady state". The "simple" genetic algorithm is described by Goldberg [62]. It is a generational algorithm in which the entire population is replaced within each generation. In the "steady state" genetic algorithm only a few individuals are replaced within each generation. This type of replacement is often referred to as overlapping populations.

Often the output values of the fitness function must be transformed in order to maintain diversity of the genetic algorithm or to differentiate between very similar individuals. The transformation from raw objective scores to scaled fitness scores is called scaling.

There are many different scaling algorithms. Some of the most common are the linear (fitness-proportionate) scaling, the sigma truncation scaling, and sharing. Linear scaling transforms the objective score based on a linear relationship using the maximum and minimum scores in the population as the transformation metric. Sigma truncation scaling uses the population standard deviation to perform a similar transformation and diminishes the poor individuals. Sharing decreases the score of individuals which are similar to other individuals in the population. For a complete description of each of these scaling methods, see Goldberg book [62].

The selection method determines how individuals are chosen for mating. If one uses a selection method which picks only the best individual, then the population will quickly converge to that individual. Thus, the selection method should be biased toward better individuals, but should allow also to pick some which aren't quite as good, but hopefully have some good genetic material. Some of the more common selection methods include the roulette wheel selection (the likelihood of picking an individual is proportional to the individual's score), the tournament selection (a number of individuals are picked using roulette wheel selection, then the best of these is (are) chosen for mating), and rank selection (pick the best individuals every time). Sometimes the crossover operator and the selection method lead to a fast convergence of the population of individuals that are almost exactly the same. If the population consists of similar individuals, the likelihood of finding new solutions typically decreases. As a result, the population becomes trapped into a local extremum. On the one hand,

it is desirable that the genetic algorithm finds "good" individuals, but on the other hand this method must maintain diversity.

One can introduce a simple physical interpretation of the genetic operators. The initial population one can interpret as "particles" on the potential surface of the problem. The problem of optimization corresponds to the search of the highest/lowest point of this surface. The mutation operation on a member of the population can be interpreted as a random fluctuation due to the interaction of a "particle", described by this individual, with a "thermal bath". The crossover operation between two individuals refers to some effective "interaction" between two "particles" described by these individuals. Starting from the initial population of "particles" at random positions, the mutation and crossover operations propagate them stochastically over the potential surface. The procedure of acceptance or rejection of the generated offsprings leads to concentration of "particles" near the extremal sites on the potential surface.

In general, genetic algorithms are much more effective than other search methods, if the search space has many local extrema. Genetic search methods have been recently applied, for example, to optimize the atomic structures of small clusters [45, 46, 47, 48]. In these studies the global minimum of the energy functional was obtained for different cluster species using Lennard-Jones potentials [45], ionic potentials [47], or interaction potentials derived from the tight-binding Hamiltonian [46, 48]. Especially successful applications of GA were performed in control theory [5].

However, in all extensions or applications of evolutionary algorithms performed up to now, including the above mentioned optimization of the clusters structure, only classical objects (position of atoms, harmonics of the pulse etc.) have been treated. The reason is that "classical" GA operators like mutation or crossover do not take care about newly generated wavefunctions which must be smooth functions. This leads to generation of "offsprings" with discontinuities at the positions of crossover or mutation operations and, therefore, having infinitely large energies. In the next subsection the first extension of a genetic algorithm to quantum problems is presented.

2.2.2 Definition of the representation, fitness and genetic operators for quantum ground-state problem

Let $\hat{H}$ be the hermitian Hamiltonian operator of a N-body quantum mechanical system:

$$\hat{H} = \hat{H}_{kin} + \hat{H}_{pot} + \hat{H}_{int}, \tag{2.29}$$

where (throughout the section we use atomic units $\hbar$=m=e=1)

$$\begin{aligned} \hat{H}_{kin} &= \frac{1}{2}\sum_{i=1}^{N}\vec{\nabla}_i^2, \\ \hat{H}_{pot} &= \sum_{i=1}^{N} U(\vec{x}_i), \\ \hat{H}_{int} &= \sum_{i=1}^{N-1}\sum_{j=i+1}^{N} V(\vec{x}_i - \vec{x}_j). \end{aligned} \tag{2.30}$$

Operators $\hat{H}_{kin}$, $\hat{H}_{pot}$, $\hat{H}_{int}$ refer to the kinetic, potential and interaction energy.

Let us first consider a quantum mechanical ground state problem for the system described by the Hamiltonian Eq. [2.29]. Let $\Psi(\vec{x}_1, \vec{x}_2, ..., \vec{x}_N)$ be an arbitrary N-body wavefunction. We assume that Ψ is normalized: $\langle\Psi|\Psi\rangle = 1$. One can write an inequality for the ground state energy E_0 in this case:

$$E_0 \leq \langle\Psi|\hat{H}|\Psi\rangle. \tag{2.31}$$

Starting with a population of the trial wavefunctions one can run the evolutionary procedure until the global minimum of the energy functional given by Eq. [2.31] is attained.

For simplicity let us first consider a ground state problem for a single particle in a one dimension. As we mentioned before, there are many different ways to prescribe the evolution of the population and the creation of the offsprings. The genetic algorithm which we propose to obtain the ground state of a quantum system can be described as follows:

(i) We create a random initial population $\{\Psi_j^{(0)}(x)\}$, $j = 1, .., N_{pop}$ consisting of N_{pop} wave functions.

(ii) The fitness function $E[\Psi_j^{(0)}]$ of all individuals is determined.

(iii) A new population $\{\Psi_j^{(1)}(x)\}$ is created through application of the genetic operators.

(iv) The fitness of the new generation is evaluated. The best new members replace the worst members from the previous population.

(v) Steps (iii) and (iv) are repeated for the successive generations $\{\Psi_j^{(s)}(x)\}$ until convergence is achieved and the ground-state wave function is found.

Usually, real space calculations deal with boundary conditions on a box. Therefore, in order to describe a wave function within a given interval in one dimension $a \leq x \leq b$ we have to choose boundary conditions for $\Psi(a)$ and $\Psi(b)$. For simplicity we set $\Psi(a) = \Psi(b) = 0$, i.e., we consider a well with infinite walls at $x = a$ and $x = b$. However, one can employ, for example, periodic boundary conditions considering a ring system [73].

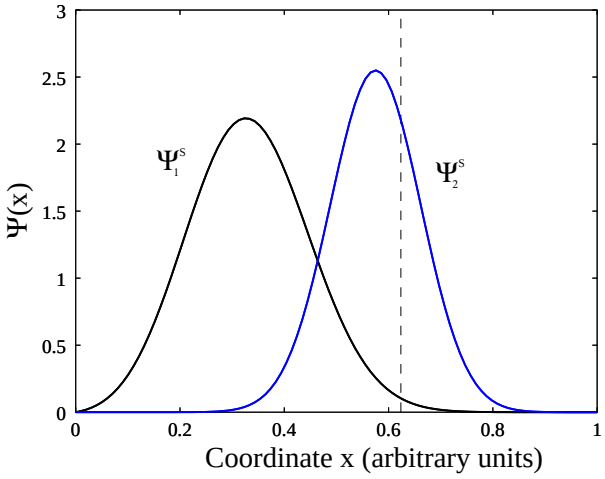

Figure 2.6: Two randomly chosen wavefunctions for the crossover operation. The vertical dashed line shows the position of the crossover.

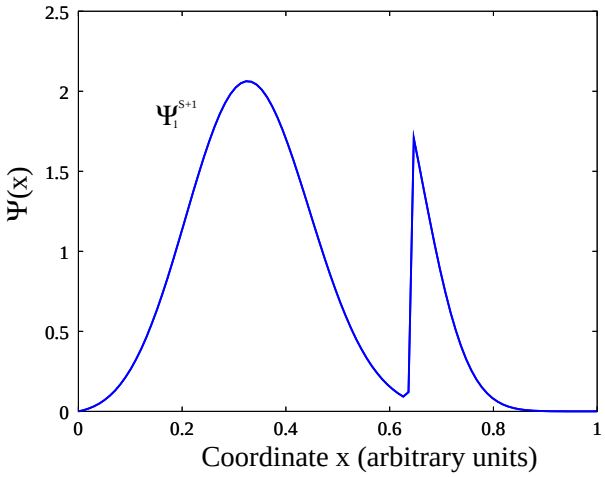

Figure 2.7: An example of the direct application of the "classical" crossover operation. Note the discontinuity of the function Ψ_1^{S+1} at the position of the crossover operation.

Inside the box one can consider different kinds of external potentials. If the size of the box is large enough, boundary effects on the results of our calculations can be minimized.

As an initial population of wave functions satisfying the boundary conditions $\Psi_j(a) = \Psi_j(b) = 0$ we choose Gaussian-like functions of the form

$$\Psi_j(x) = A_j \ \exp(-(x - x_j)^2/\sigma_j^2)(x - a)(b - x), j = 1, .., N_{pop}, \qquad (2.32)$$

with random values for the peak position $x_j \in [a, b]$ and the width $\sigma_j \in (0, b-a]$. The amplitudes A_j are determined from the normalization condi-

tion $\int_a^b |\Psi(x)|^2 dx = 1$ for given values of x_j and σ_j. One can significantly

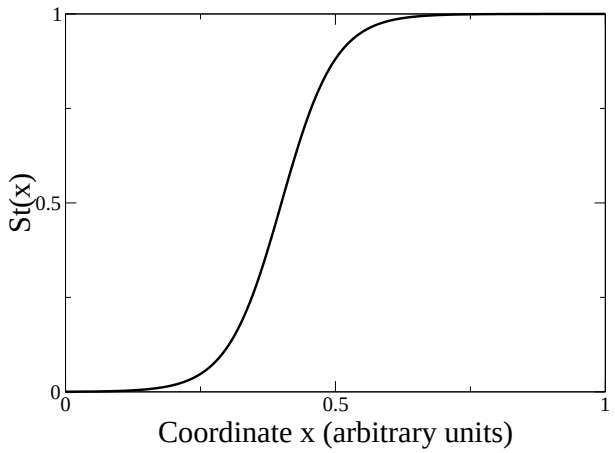

Figure 2.8: An example of a smooth step function $St(x)$ used in the crossover operation. $x_0 = 0.4$, $k_c = 0.1$ (see text).

reduce computational costs choosing a proper form of initial wavefunctions. If any approximate form of the solution is known, one can generate random initial population "near" this solution. After a few iterations successful offsprings will converge to the improved solution. It also seems useful to generate an initial population with the symmetry properties, reflecting the symmetry of the Hamiltonian. However, we shall show that the QGA successfully finds solutions starting from a population defined by Eq. [2.32].

As we mentioned above, we should define three kinds of operations on the individuals: the copy, the mutation of a wavefunction, and the crossover between two wavefunctions (see Fig.[2.6]). While the copy operation has the same meaning as in previous applications of the GA, both the crossover and the mutation operations have to be redefined for application to the quantum mechanical case. The reason is that after straightforward application of crossover operation between two "parents" one unavoidably obtains both "children" with discontinuities at the position of crossover.

This implies that "offsprings" have an infinite (practically, very large) kinetic energy, and therefore, cannot be considered as good candidates to be the ground state wavefunction (see Fig. [2.7]).

To avoid this problem we suggested a new modification of the genetic operations for application to smooth and differentiable wavefunctions. The smooth crossover is defined as follows. Let us take two randomly chosen "parent" functions $\Psi_1^{(s)}(x)$ and $\Psi_2^{(s)}(x)$ (see Fig.[2.6]). We can construct two new functions $\Psi_1^{(s+1)}(x), \Psi_2^{(s+1)}(x)$ as

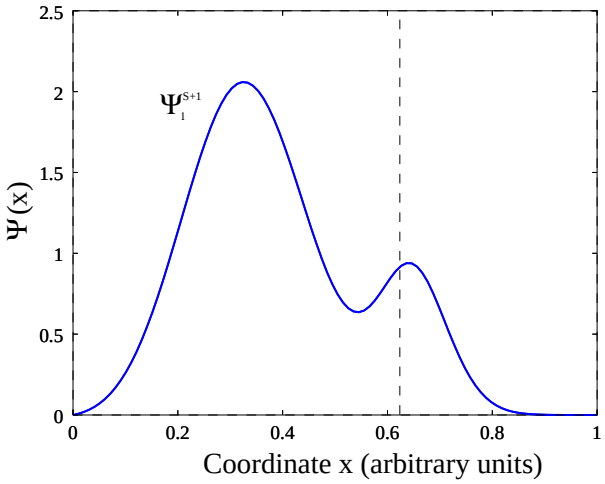

Figure 2.9: An example of the application of the "smooth" crossover operation. The vertical dashed line shows the position of the crossover operation.

$$\begin{aligned} \Psi_1^{(s+1)}(x) &= \Psi_1^{(s)}(x)\ St(x) + \Psi_2^{(s)}(x)\ (1 - St(x)) \\ \Psi_2^{(s+1)}(x) &= \Psi_2^{(s)}(x)\ St(x) + \Psi_1^{(s)}(x)\ (1 - St(x)), \end{aligned} \tag{2.33}$$

where $St(x)$ is a smooth step function involved in the crossover operation. We consider $St(x) = (1 + \tanh((x - x_0)/k_c^2))/2$, where x_0 is chosen randomly ($x_0 \in (a, b)$) and k_c is a parameter which allows to control the sharpness of the crossover operation. The function St(x) is shown in Fig [2.8]. The result of the smooth crossover is presented in Fig. [2.9] In the limit $k_c \to 0$ one obtains the usual Heaviside step function $St(x) = \theta(x - x_0)$ and Eqs. [2.33] become the "classical" crossover operations. Note, that the crossover operation does not violate the boundary conditions and application of the crossover between identical wavefunctions generating the same wavefunctions.

The mutation operation in the quantum case must take into account also the smoothness of the generated wavefunctions. It is not possible to change randomly the value of the wave function at a given point without producing dramatic changes in the kinetic energy of the state. To avoid this problem we define the mutation operation as

$$\Psi^{(s+1)}(x) = \Psi^{(s)}(x) + \Psi_r(x), \tag{2.34}$$

where $\Psi_r(x)$ is a random mutation function. In the presented work we choose $\Psi_r(x)$ as a Gaussian-like function $\Psi_r(x) = B \exp(-(x_r - x)^2/k_m^2)(x - a)\ (b - x)$ with a random center $x_r \in (a, b)$, width $k_m \in (0, b - a)$, and a

small amplitude B which can be both positive or negative. The so defined mutation does not violate the boundary conditions.

In order to find the ground state, for each step of the QGA iteration we randomly perform copy, crossover and mutation operations. After each application of the genetic operation (except coping) the new-created functions are normalized. For the extension of the QGA in order to treat quantum systems in two dimensions see Appendix C. We have used $P_m = 0.03$ for the probability of a mutation and $P_c = 0.97$ for the probability of a crossover operation. During our calculations we set different sizes of the population N_{pop} up to 1000. However, the population size of only 200 parents usually guarantees a good convergence of the algorithm.

In our approach a wavefunction $\Psi(x)$ is discretized on the mesh $\{x_i\}$,$i = 1, .., L$, where L is a number of discretization points, and represented by the genetic code vector $\Psi(x_i)$.

2.2.3 Extension of the QGA for the solution of quantum statistical problems

In order to compute not only a ground state, but also exited states one needs a further extension of the QGA. For this purpose we use a variational formulation for the partition function Z of many-body quantum system.

Let $\{\Psi_k\}$ be an arbitrary orthonormal set of M N-body wave functions ($\Psi_k = \Psi_k(\vec{x}_1, .., \vec{x}_N), k = 1..M$). It can be shown that the partition function Z of the quantum system satisfies the following inequality [61]:

$$Z \geq Z' \equiv \sum_{k=1}^{M} e^{-\beta \langle \Psi_k | \hat{H} | \Psi_k \rangle}, \tag{2.35}$$

where the Hamiltonian $\hat{H}$ is defined by Eq. [2.29] and parameter β is proportional to the inverse temperature: $\beta = \frac{1}{k_B T}$, where k_B is the Boltzmann constant. The equality holds only if $\{\Psi_k\}$ is the complete set of eigenfunctions of the Hamiltonian $\hat{H}$. Note, that $\{\Psi_k\}$ does not have to be a complete set. In practice, for finite temperatures calculations using Eq. [2.35], one can take into account the lowest M levels of the system, neglecting the occupation of the levels with a higher energy. The number of considered levels M can be chosen in such way, that occupation of the neglected levels does not exceed a certain value for a given temperature. In the limit the temperature T goes to zero ($T \to 0$ or $\beta \to +\infty$) one can neglect all terms in Eq. [2.35] except the largest one (let it be the term containing Ψ_1). In this case Eq. [2.35] becomes equivalent to the variational principle for the ground state energy E_0:

$$E_0 \leq \langle \Psi_1 | \hat{H} | \Psi_1 \rangle. \tag{2.36}$$

Following the spirit of the QGA we assume that each member of the population represents the set of M trial orthonormal wavefunctions $\{\Psi_k\}$. According to Eq [2.35] one can obtain eigenfunctions of the Hamiltonian $\hat{H}$ and also the partition function Z by running an evolutionary procedure until the sum in Eq. (2.35) attains its maximum possible value.

In practice, full quantum mechanical calculations of the excitation spectrum are quite difficult to perform even for the case of very few interacting particles. The reason is the huge data amount rapidly increases with the number of particles considered in the system [38]. Therefore, quantum mechanical calculations with exact many body wave function are limited to 3-4 particles.

For a simplified study of the problem, we reduce the dimension of the many particle wavefunction Ψ using the Hartree-Fock approximation. This is the simplest way to account for electron-electron interactions within the quantum system [87]. The Hartree-Fock level is implemented across nuclear and atomic physics as a first step towards solution of the quantum many-body problem [64].

Let us consider a system of N spinless particles occupying K one particle states (N≤K). For such a system one can construct $M = \frac{K!}{N!(K-N)!}$ N-particle wavefunctions $\Psi_k(\vec{x}_1, ..\vec{x}_N)$, $1 \leq k \leq M$, corresponding to all possible configurations. The N-particle wavefunction is represented by the Slater determinant:

$$\Psi_k(\vec{x}_1, ..\vec{x}_N) = \frac{1}{\sqrt{N!}} \begin{vmatrix} \psi_{i_1}(\vec{x}_1) & \psi_{i_1}(\vec{x}_2) & \dots \\ \psi_{i_2}(\vec{x}_1) & \psi_{i_2}(\vec{x}_2) & \dots \\ \vdots & \vdots & \ddots \end{vmatrix}. \tag{2.37}$$

Where indexes $1 \leq i_1, i_2, ..., i_N \leq K$ counts the one particle states in the state k. This means that the set $\{\Psi_k\}$ will represent the exact excitation states for the case of noninteracting particles. For the interacting case $\{\Psi_k\}$ will correspond to the Hartree-Fock approximation. For simplicity let us consider one dimensional problems. However, generalization of the presented algorithm to higher dimensions is straightforward. As in the case of searching for the ground state, we perform calculations on a finite region $[a, b]$ where we discretize the real space.

The algorithm is implemented as follows. An initial random population of N_{pop} trial sets of one-particle wave-functions $\{\psi_i^j\}$, where the index j counts each member of the population: $j = 1, .., N_{pop}$, and the index i counts one-particle wave-functions: $i = 1, .., K$. For this purpose we construct $K \times N_{pop}$ one particle wavefunctions ψ_i^j using a Gaussian-like form

$$\psi_i^j(x) = A_i^j \ \exp\big(-(x - \bar{x}_i^j)^2/{\sigma_i^j}^2\big)\ (x-a)\,(b-x), \tag{2.38}$$

and index j denotes that the one particle wavefunction $\psi_i^j(x)$ belongs to the member with index j. We generate random values $\bar{x}_i^j \in (a, b)$, and

$\sigma_i^j \in (0, b-a]$ for each one particle wavefunction. The defined in such way wavefunctions $\psi_i^j(x)$ fulfill zero conditions on the boundaries. All one-particle wave functions $\{\psi_i^j\}$ which belong to the same member j are orthogonalized and normalized for the initial population, and then ordered in respect to their energy expectation value.

As in the case of searching for the ground state, offsprings of the initial generation are formed through application of genetic operators on the genetic codes. As in previous cases, we define "quantum" analogies of three kinds of genetic operations on the individuals: the copy, the mutation, and the crossover.

For each iteration of the QGA procedure we randomly perform copy, crossover and mutation operations, applied to one particle wavefunctions $\psi_i^j(x)$. The crossover operations are applied between randomly chosen one particle wave functions $\psi_i^{j_1}(x)$ and $\psi_i^{j_2}(x)$ (members j_1 and j_2 respectively) corresponding to the same one-particle excitation state i.

The fitness function, i.e. the functional to be maximized by the QGA, is the sum Z' defined in Eq. (2.35). After each application of a genetic operation the new-created one particle wavefunctions are normalized and orthogonalized. Then, the fitness of each new member is evaluated and the fittest members are selected. The procedure is repeated until convergence of the fitness function to the optimal value is reached.

Maximizing Z', one obtains the "best" set of the excitation spectrum $\{\Psi_k\}$ for a given system. Then one can use this set in order to compute any kind of quantum statistical values, for example, the density of particles $\rho(x)$ for any value of the parameter β (see [65]):

$$\rho(x) = \rho(\beta, x_N) = \int_a^b \rho(\beta, \mathbf{x}) dx_1 ... dx_{N-1},$$

where $\rho(\beta, \mathbf{x})$ is given by

$$\rho(\beta, \mathbf{x}) = \frac{\sum_k \exp(-\beta \langle \Psi_k(\mathbf{x}) | \hat{H} | \Psi_k(\mathbf{x}) \rangle) |\Psi_k(\mathbf{x})|^2}{\sum_k \exp(-\beta \langle \Psi_k(\mathbf{x}) | \hat{H} | \Psi_k(\mathbf{x}) \rangle)},$$

and here we use notation $\mathbf{x} = \{x_1, ..., x_N\}$.

2.3 Photon assisted tunneling between quantum dots: optimal control approach

In this section we investigate optimal control of the carrier dynamics in nanostructures. As a model device we consider an electron pump based on resonant photon-assisted tunneling through a double quantum dot [95]. We search for the shape of the optimal control field in order to maximize the transfered charge in the system.

In the first subsection a physical picture and equations of motion in terms of density matrix are given.

In the second subsection we formulate the control problem that is reduced to the control of a time averaged current between two quantum dots. In this paragraph we also describe the method that we employed for the numerical solution.

2.3.1 Equations of motion in terms of density matrix

We consider a double quantum dot device coupled to two metallic contacts (reservoirs) and configured as an electron pump as described in Ref. [95]. This device is illustrated in Fig. [2.10]. The double quantum dot can be modeled by only two non-degenerate and weakly coupled electron levels with energies ε_1 and ε_2. By sweeping the gate voltages one can vary $\Delta\varepsilon = \varepsilon_2 - \varepsilon_1$.

The bonding and antibonding states, which are a superposition of the wavefunctions corresponding to an electron in the left or in the right dot, have an energy splitting of $\Delta E = E_{antibonding} - E_{bonding} = \sqrt{\Delta\varepsilon^2 + 4d^2}$ where d is the tunnel coupling between the two dots.

The quantum dot 1 is connected to the reservoir on the left, and the second quantum dot is coupled to the right reservoir. The applied voltage is biased in such a way that the chemical potential of the left reservoir μ_R is lower than that on the right reservoir μ_L. Therefore, in absence of external perturbation the level 1 is occupied whereas level 2 is empty. Since we also assume that the coupling between the quantum dots is very weak, no current flows in the absence of external fields.

If an external resonant electric field is applied to the system, it works as a pump: Rabi oscillations of the electron occupations occur between the levels 1 and 2, and electrons can tunnel from the left to the right reservoir [95, 96].

The Hamiltonian of the double QD coupled to the external field can be expressed as

$$H_{DQD} = \sum_{i=1}^{2} \varepsilon_i(t)\, c_i^+ c_i + d\,(c_1^+ c_2 + c_2^+ c_1), \tag{2.41}$$

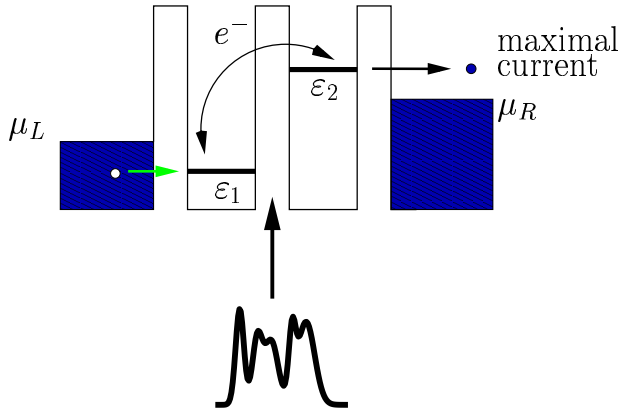

Figure 2.10: Illustration of the "electron pump" device: two quantum dots coupled to contacts. Electron can tunnel from the left contact to the left quantum dot. If the resonant control field is applied the electron can jump to the right quantum dot and it can further tunnel to the right contact.

where c_i^+ (c_i) is the creation (annihilation) operator for an electron on dot i and the diagonal matrix elements are given by $\varepsilon_i(t) = (-1)^i/2\ (\Delta\varepsilon + V(t)\cos\omega t)$. $V(t)\cos\omega t$ is the time-varying external field, which causes the on-site energies to oscillate against each other. The amplitude $V(t)$ is also time-dependent and describes the pulse shape.

The Hamiltonian for the metallic reservoirs and the tunnel barriers is given by [95]

$$\begin{aligned} H_{RT} &= \sum_{\mathbf{k},\ell=L,R} \varepsilon_{\mathbf{k}\ell}\, c_{\mathbf{k}\ell}^+ c_{\mathbf{k}\ell} + \sum_{\mathbf{k}} W_{\mathbf{k}L}\, (c_{\mathbf{k}L}^+ c_1 + c_1^+ c_{\mathbf{k}L}) \\ &\quad + \sum_{\mathbf{k}} W_{\mathbf{k}R}\, (c_{\mathbf{k}R}^+ c_2 + c_2^+ c_{\mathbf{k}R}) + U n_1 n_2. \end{aligned} \tag{2.42}$$

Here, $c_{\mathbf{k}\ell}^+$, with $\ell = L, R$ creates an electron of momentum $\mathbf{k}$ in reservoir ℓ. The quantities $W_{\mathbf{k}\ell}$, with $\ell = L, R$ represent the tunnel matrix elements between the reservoirs and the QDs. U is the magnitude of the interdot electron-electron repulsion, and the occupation operators n_1 and n_2 are given by $n_1 = c_1^+ c_1$ and $n_2 = c_2^+ c_2$. For simplicity, the electron spin is neglected.

In the derivation of equations of motion we have used the following approximation. We assume that the reservoir on the right has a broad band of unoccupied states, so that after an electron has jumped from the second quantum dot to the right reservoir it cannot jump back. Thus, the time scale for the tunneling process between the second dot and the reservoir on the right is determined by a transfer rate $\Gamma_2 = 2\pi\rho_R(\varepsilon)|W_{\mathbf{k}R}|^2$, where ρ_R is the density of states in the right reservoir. Similarly, the transfer rate to the left contact Γ_1 is given by $\Gamma_1 = 2\pi\rho_L(\varepsilon)|W_{\mathbf{k}L}|^2$.

In order to describe the electron dynamics we use a density matrix approach similar to that was derived in [54]. For the given above Hamiltonian, the master equation for the density matrix $\rho(t)$ which describes the evolution of the system reads

$$\begin{aligned} i\hbar\frac{\partial}{\partial t}\rho_{11} &= i\Gamma_1\rho_0 + d(\rho_{12}-\rho_{21}), \\ i\hbar\frac{\partial}{\partial t}\rho_{22} &= -i\Gamma_2\rho_{22} + d(\rho_{21}-\rho_{12}), \\ i\hbar\frac{\partial}{\partial t}\rho_{12} &= -i\frac{\Gamma_2}{2}\rho_{12} + 2\varepsilon_1(t)\rho_{12} + d(\rho_{22}-\rho_{11}), \\ i\hbar\frac{\partial}{\partial t}\rho_{21} &= -i\frac{\Gamma_2}{2}\rho_{21} + 2\varepsilon_2(t)\rho_{21} + d(\rho_{22}-\rho_{11}). \end{aligned} \tag{2.43}$$

Eqs. (2.43) allow to investigate the case of zero and infinite interdot Coulomb repulsion U by choosing the proper expression for the quantity ρ_0. For $U = 0$ we put $\rho_0 = 1 - \rho_{11}$, whereas the case $U \to \infty$ requires $\rho_0 = 1 - \rho_{11} - \rho_{22}$, which projects out double occupancies [54]. The initial situation is $\rho_{11} = 1$, $\rho_{22} = 0$, as can be inferred from Fig.[2.10]. We consider photon assisted tunneling if the one-photon resonance condition $\hbar\omega = \sqrt{\Delta\varepsilon^2 + 4d^2}$ is satisfied.

Equations Eqs. [2.43] can be solved analytically for certain limiting cases. For instance, considering only an isolated system of two QD's ($\Gamma_1 = \Gamma_2 = 0$) in an electric field, periodic in time and with a constant amplitude $V(t) = V_0$, an electron placed on one of the dots will oscillate back and forth between the dots with the Rabi frequency ω_R:

$$\omega_R = \frac{2d}{\hbar} J_N(\frac{V_0}{\hbar\omega}), \tag{2.44}$$

where J_N is the Bessel function of order N. N refers to the number of photons absorbed by the system in order to fulfill the resonance condition $N\hbar\omega = \sqrt{\Delta\epsilon^2 + 4d^2}$.

2.3.2 The control problem

From the integration of Eqs. (2.43) one obtains the charge transferred from the left into the right reservoir due to the action of the external field over a finite time interval $[0, T]$. For that purpose we write the current operator $\hat{J} = id/\hbar\,(c_1^+\,c_2 - c_2^+\,c_1)$ which leads, in combination with Eqs. (2.43) to the time dependent average current

$$\langle I(t)\rangle = e\,Tr\left\{\hat{\rho}\,\hat{J}\right\} = e\frac{\partial\rho_{22}(t)}{\partial t} + \frac{e\,\Gamma_2}{\hbar}\,\rho_{22}(t), \tag{2.45}$$

where e is the electron charge and Tr is the trace operation. The net transferred charge from left to the right QD Q_T is obtained as

$$Q_T = \int_0^T dt\,\langle I(t)\rangle = \frac{e\,\Gamma_2}{\hbar}\int_0^T dt\,\rho_{22}(t) + e\,\rho_{22}(T)\,. \tag{2.46}$$

Obviously, Q_T only represents the transferred charge to the right reservoir only if $\Gamma_2 \neq 0$. The second in Eq. [2.46] term indicates that, after the field is switched off ($t > T$, the charge remaining in the second quantum dot $e\,\rho_{22}(T)$ is completely transferred to the right reservoir.

It is important to point out that $Q_T = Q_T[V(t)]$ is a nonlinear functional of the field amplitude $V(t)$, and can exhibit different types of behavior depending on the form of $V(t)$. For instance, if the external field has a Gaussian shape $V(t) = V_0 \exp(-t^2/2\tau^2)$ of duration τ, then Q_T shows Stückelberg-like oscillations as a function of τ[96]. However, the Gaussian shape of $V(t)$ does not necessarily maximize the transferred charge. Our goal is to find the optimal pulse shape $V_{opt}(t)$ which maximizes Q_T, i.e., which satisfies $Q_T^{max} = Q_T[V_{opt}(t)]$.

The problem of finding $V_{opt}(t)$ is very complicated due to its high nonlinearity and the large number of degrees of freedom. Therefore, we use the genetic algorithm (GA) as a global search method.

In our present approach the vector representing the genetic code is just the pulse shape $V(t)$ discretized on a time interval $t \in [0, T]$. The fitness function, i.e. the functional to be maximized by the successive generations is the transferred charge $Q_T[V(t)]$ (see Eq. [2.46]. The genetic algorithm applied to pulse shaping consists of the following steps:

(i) We create a random initial population $\{V_j^{(0)}(t)\}$, $j = 1, \ldots, N$, consisting of N different pulse amplitudes $V_j^{(0)}(t)$.

(ii) The fitness function $Q_T[V_j^{(0)}(t)]$ of all individuals is determined.

(iii) A new population $\{V_j^{(1)}(t)\}$ is created through application of the genetic operators.

(iv) The fitness of the new generation is evaluated.

(v) Steps (iii) and (iv) are repeated for the successive generations $\{V_j^{(n)}(t)\}$ until convergence is achieved and the optimal pulse shape which maximizes Q_T is found. We implement the same realization of the GA as in the Theory section [2.2].

We assume that the control field is active within a time interval [0,T] with boundary conditions $V(0) = V(T) = 0$. As initial population of field amplitudes satisfying the boundary conditions we choose Gaussian-like functions of the form

$$V_j^{(0)}(t) = I_j^0 \ \exp(-(t - t_j)^2/\tau_j^2)\ t\,(t - T), \tag{2.47}$$

with random values for the position of the maximum $t_j \in [0, T]$ and the duration $\tau_j \in (0, T]$. The peak amplitude I_j^0 for each pulse is calculated from the condition that all pulses must carry the same energy

$$E = \int_0^T V^2(t)\ \cos^2(\omega t) dt. \tag{2.48}$$

Eq. (2.48) represents a constraint for our calculations. One could consider the value of the pulse energy E also as a parameter to be optimized.

The above formulated control problem (Eqs. [2.43,2.46,2.48] is applied to a rather simple quantum system. However, as we shall see, the optimal control fields have a nontrivial shape and induce a complicated dynamics of the electron occupations in the system.

2.4 Explosion of noble gas clusters in strong laser fields

In this section we give a theory in order to describe the explosion of Xe clusters interacting with very strong femtosecond laser fields. Because the strength of the laser field is comparable with the Coulomb attraction of an electron to an nucleus in the Hydrogen atom, this excludes the possibility of a perturbative treatment of the problem.

In the first subsection we describe the main time and length scales and physical quantities that characterize the cluster explosion process. This analysis helps us to derive a physically relevant and computationally tractable model.

In the second subsection possible mechanisms of ionization and explosion are discussed.

In the third paragraph equation of motion for electrons and nuclei are given. In our model we treat electrons quantum mechanically using density functional approach. The point-like nuclei are described classically.

In the forth paragraph a short sketch of the implemented numerical methods is given.

2.4.1 Time and length scales for the cluster explosion

Let us discuss the time scales that characterize the main processes during the cluster explosion. The fastest process is represented by the electron dynamics inside the atoms. It is characterized by the fundamental atomic time scale:

$$t_{au} = \frac{2m_e a_0}{\hbar}, \tag{2.49}$$

where m_e is electron mass and a_0 is atomic Bohr radius. Using Eq. [2.49] one can estimate that relevant electron dynamics happens on time scales of $t_{au} = 2.27 \times 10^{-1}$ fs. Another characteristic time scale corresponds to the period of the laser field oscillations. Because in experiments mostly a $Ti : sapphire$ laser with wavelengths in the range of $620 - 840$ nm is used, the period of oscillation can be estimated as $t_l = \lambda/c \approx 2$ fs. The next time scale is related to the ionization process that occurs mainly during the first $5 - 50$ optical cycles [60]. The laser pulse duration represents a very significant time scale that is usually in the range of $20 - 800$ fs. The largest time scale in the considered problem is defined by a motion of heavy nuclei. The correspondent times are of the order of $100 - 1000$ fs. In order to make realistic quantum mechanical calculations one has to take into account all above mentioned time scales (see Fig. [2.11]).

Let us now estimate the length scales involved in the cluster explosion. The smallest length scale is defined by the De Broglie wavelength λ_{DB} of

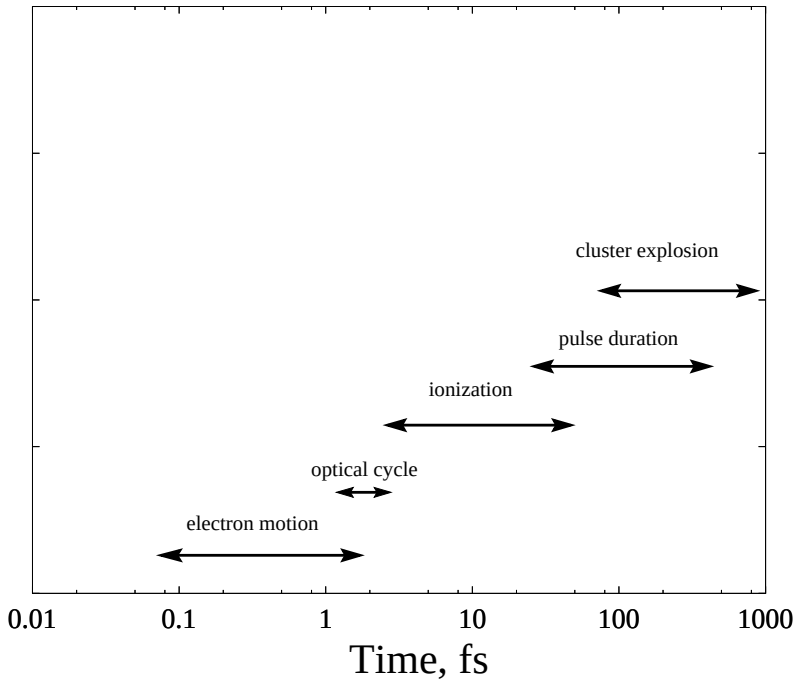

Figure 2.11: Main time scales (in femtoseconds) involved in a cluster explosion.

the most energetic electrons:

$$\lambda_{DB} = \sqrt{\frac{2\pi\hbar^2}{m_e E_{kin}}}, \tag{2.50}$$

where E_{kin} is the kinetic energy of electrons. Substituting in Eq. [2.50] the typical kinetic energy $E_{kin} \approx 3$ keV of ejected electrons observed in experiments [55] one obtains $\lambda_{DeB} \approx 0.25\, a_0$. This means that for such energetic electrons a classical treatment is relevant because their wavelength is considerably smaller than the internuclei spacing d, which is typically $d = 8.5\, a_0$ for Xe clusters [17].

However, if one wants to describe the ionization, that is essentially a quantum mechanical process, one needs to use a quantum treatment and to make very fine discretization of the real space with $\Delta x \ll \lambda_{DeBroglie}$ in order to account for such energetic electrons. The size of the clusters we are interested in, is in the range of $10\, a_0 - 100\, a_0$. This corresponds to approximately $100-2500$ atoms in the cluster. In order to make real space calculations, one needs to define a certain region (box). This box should be large enough in order to make the border effects negligible. Because of the explosion process the size of the box L should be at least ten times larger than initial size of the cluster: L is in the range of $100a_0 - 1000a_0$ (see Fig. [2.12]). The wavelength of the laser field is typically few hundreds

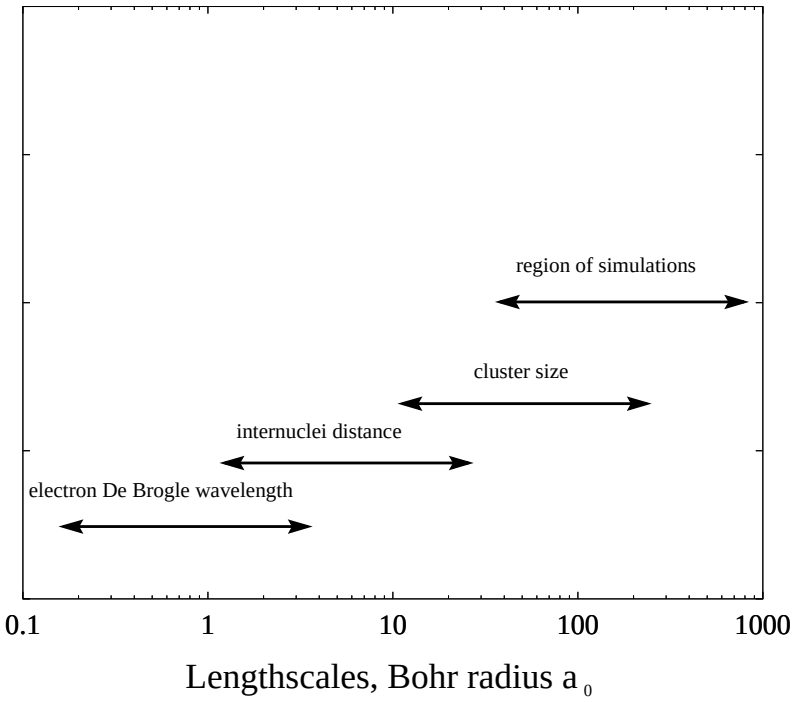

Figure 2.12: Main length scales involved in cluster explosion.

of nanometers and hence significantly larger than all above mentioned lengthscales. Therefore we assume in our simulations a uniform laser field.

The regime of fast and energetic excitations in cluster explosion experiments [15, 16, 17] goes far beyond any peturbative treatment. For example, the laser pulse with a peak intensity $3.16 \times 10^{16}\mathrm{W/cm}^2$ corresponds to the Coulomb field strength experienced by an electron in the ground state of atomic Hydrogen. This requires a fully nonadiabatic description of both electronic and ionic response.

2.4.2 Explosion scenario

The physical scenario for cluster explosion which emerges from the different experimental observations and calculations can be divided into 3 stages:

(1) The laser pulse excites electrons into states of very high kinetic energy. Thus, both ionization and expansion of the cluster occur. Because of the very strong external field, high-order multiphoton ionization and strong electric field tunnel ionization are possible.

One can specify two types of ionization processes: inner ionization and outer ionization. Inner ionization corresponds to the removal of electrons from their host atoms (ions) so that it determines the charge q_i of the

cluster ions. Note that inner ionization does not necessarily imply that the electron leaves the cluster.

Outer ionization is manifested by electron removal from the cluster to infinity so that it determines the total cluster charge Q. The complete simulation of the ionization process has to treat both inner and outer ionization since they affect each other [31] .

(2) During the expansion the cluster can reach a certain critical radius for which the absorption of energy is particularly favored. There are two main mechanism which are responsible for the enhanced ionization. The first mechanism corresponds to the so called microplasma model [55]. Excited electrons are treated as a small spherical plasma with characteristic plasmon frequency

$$\omega_{pe} = \Big(\frac{n_0 e^2}{3 m_e \epsilon_0}\Big)^{1/2}, \tag{2.51}$$

where n_0 is electron plasma density, e is elementary charge of electron and ϵ_0 is vacuum permittivity constant. When the charged cluster starts to expand, the plasmon frequency becomes resonant with the laser frequency [22, 23, 29] that leads to very effective heating of electrons in the cluster. The second possibility is so called "ignition mechanism". In this case the lowering of the Coulomb potential that attracts electrons to one ion, by the Coulomb attraction due to its neighboring ions, enhances the rate of the over-the-barrier ionization.

As was shown by Rost and coworkers in [33] this mechanism also exhibits resonant features, i.e it becomes especially efficient for a certain internuclei distance. Because both resonances occur approximately at the same stage of explosion, it is difficult to distinguish these two mechanisms using available experimental data. If the external field is still large when resonance conditions are satisfied, then an enormous increase in the energy absorption occurs, which leads to the emission of a large fraction of electrons of the cluster.

(3) The final stage is the destruction of the cluster involving production of highly charged and highly energetic ions, which show an interesting dependence on the initial cluster radius. For cluster size more than 60nm, that corresponds to approximately 2500 atoms in the cluster, the measurements indicate highly energetic ions with energy up to 1 MeV (see Fig [1.1]) [16, 55].

There are two conventional mechanisms responsible for the ion acceleration. The first one corresponds to the case when the loss of electrons will lead to a charge buildup Q on the cluster surface that can be associated with the Coulomb pressure on the sphere with the radius r: $P_C = \frac{Q^2}{2(4\pi)^2 \epsilon_0 r^4}$. Because of the mutual repulsion between the ions the cluster becomes unstable and Coulomb explosion occurs.

The second mechanism is associated with the pressure of the hot elec-

trons (microplasma model). It is assumed that expanding electron plasma accelerates cold heavy ions. It is possible to compare the Coulomb pressure to the hydrodynamic pressure $P_H = n_e(r)k_bT_e(r)$.

Suppose that the radial velocity of the expanding cluster with electron plasma density $n_e \propto r^{-3}$ reaches a constant value shortly after the laser pulse, the plasma temperature $T_e(r) \propto r^{-1}$ solves the hydrodynamic differential equation for the electron density [17]:

$$\frac{\partial T_e}{\partial t} = -\frac{2T_e}{r}\frac{\partial r}{\partial t}. \tag{2.52}$$

This implies that P_C and P_H will be competing over a long expansion time, since they both decrease with $1/r^4$.

In experiment made by Lezius and coworkers [17] the distribution of emitted Xe^{q+} ions as a function of their kinetic energy E_{kin} and charge q were measured with high accuracy. The production of measured highly energetic ions were partially associated with the hydrodynamic mechanism. This misleading conclusion were made on a base of "linear" dependence between the kinetic energy E_{kin} and the charge state q of the atom (see Fig. [1.2]). It seems, that the authors of Ref. [17] did not mention that for distributions plotted in Fig. [1.2] the logarithmic scale for the energy has been used. And correct conclusion should be that $\log(E_{kin}) \propto q$. Therefore, we conclude that the cluster explosion mechanism is not understood well.

For the understanding of all three stages a microscopic description of the interplay between the quantum dynamics of the electrons and the ionic motion is necessary. So far, no such microscopic description has been achieved without significant simplification of the theoretical model. Moreover, a unified theoretical description of the above mentioned stages and a consistent explanation of all experiments is still lacking.

Therefore, one need a model which describes the response of a cluster to intense radiation fields by simultaneous solution of the quantum-mechanical equations of motion for the electrons and the classical equations of motion for the nuclei. Rather than computing the time evolution of a many-electron wave function, a task which at present is computationally infeasible, our theory deals with the time evolution of the electronic density under the influence of nuclear attraction, electronic repulsion, and the external radiation field. Such density-functional approaches have a rigorous foundation only for the treatment of ground-state total electronic energies [41], although some promising work has been done on time-dependent problems as well [42].

2.4.3 Equations of motion

In this subsection we present our theoretical approach. We characterize all electrons in the Xe_N cluster by the electronic density $\rho(\mathbf{r}, t) = |\psi(\mathbf{r}, t)|^2$,

with the normalization condition $\int |\psi(\mathbf{r},t)|^2\, d\mathbf{r} = N_{el}$, where N_{el} is the total number of electrons in the cluster. The quantum dynamics of $\rho(\mathbf{r})$ is coupled to the classical equations of motion for the nuclei. Thus, using atomic units, the time evolution of the cluster is described by the equations

$$i\frac{\partial\psi}{\partial t} = \left(-\frac{1}{2}\nabla^2_{\mathbf{r}} + U_{en} + U_{laser} + U_{ee} + U_{xc}\right)\psi, \tag{2.53}$$

and

$$M\ddot{\mathbf{R}}_j = -\vec{\nabla}_{\mathbf{R},j}\, \mathcal{H}_{ion}(|\psi|^2,\, \{\mathbf{R}_k\}, t). \tag{2.54}$$

Here, $\{\mathbf{R}_j\}$, $(j = 1, \ldots, N)$, are coordinates of the nuclei, M refers to the mass of the nucleus. In Eq. [2.53] $U_{en}(\mathbf{r})$ and $U_{laser}(\mathbf{r},t)$ refer to the potentials arising from the positive nuclei and the external laser field, while $U_{ee}(\mathbf{r})$ and $U_x(\mathbf{r})$ describe the Coulomb repulsion between electrons and the exchange-correlation potential, respectively.

Since laser fields used in cluster explosion experiments have a linear polarization of the light, we assume that all particles in the system move in one spatial dimension along the vector of the polarization. The one dimensional approximation has been used extensively in the treatment of strong-field interactions with atoms and small clusters [28], and in such cases it reproduces qualitatively many key phenomena encountered in three-dimensional systems. It is perhaps better justified for the treatment of small molecules which tend to become quickly aligned with the polarization vector of the field, than for clusters treated here, which display essentially isotropic dissociation [55]. However, we adopt this approximation in order to make the necessary computations tractable.

With this restriction, the potential U_{en} appearing in Eq. [2.53] is given by

$$U_{en}(x) = -\sum_{i=1}^{N} \frac{Q}{\sqrt{(x - R_i(t))^2 + a^2}}, \tag{2.55}$$

where $Q = 54$ for Xenon, and the (Hartree-like) Coulomb repulsion between electrons U_{ee} is described by

$$U_{ee}(x) = \frac{1}{2}\int dx' \frac{|\psi(x',t)|^2}{\sqrt{(x-x')^2 + b^2}}. \tag{2.56}$$

In Eqs. [2.55] and [2.56], a and b are smoothing parameters to eliminate the singularity at x=0, while retaining the long-range character of the interactions. Using $a = 2.5\ a_0$ and $b = 3.4\ a_0$ we reproduce the experimental equilibrium internuclear separation of the Xe_2 molecule and binding energy of 0.048 eV. The external laser field acting on the electrons is given by $U_{laser}(x,t) = A(t)\, x\, \sin(\omega t)$, where $A(t)$ is the envelope of the laser pulse with frequency ω. In Eq. [2.53] we use the simplest form of the exchange-correlation functional $U_{xc}(x) = -3/4\,(3/\pi)^{\frac{1}{3}}\,|\psi(x,t)|^{\frac{2}{3}}$ which one

can obtain considering the non-interacting uniform electron gas. Finally, the Hamiltonian $\mathcal{H}_{ion}$ for the nuclei is given by

$$\mathcal{H}_{ion} = \sum_{j=1}^{N} \frac{P_j^2}{2M} + \sum_{j=1}^{N-1} \sum_{k=j+1}^{N} \frac{Q^2}{\sqrt{(R_k - R_j)^2 + a^2}}$$
$$+Q \int U_{en}(x)\ |\psi(x,t)|^2 dx - Q \sum_{j=1}^{N} R_j\, A(t)\ \sin(\omega t), \tag{2.57}$$

where the different terms describe the kinetic energy, the Coulomb repulsion between nuclei, the electron-ion attraction, and the coupling of the ions to the external laser field, respectively.

2.4.4 Integration of the equations of motion: the split operator method

In order to integrate Eq. [2.53] having the form

$$i\frac{\partial}{\partial t}\Psi = \hat{H}\Psi, \tag{2.58}$$

we applied an accurate and efficient technique that is called the split operator method. This technique was successfully applied to quantum dynamics problems [67]. In the following we describe the main idea of the method.

Let us consider first the representation of the wavefunction and operators on the interval $x \in [x^{min}, x^{max}]$. We consider equidistant grids that are defined as follows:

$$x^j = x^{min} + (j-1)\Delta x, j = 1, ..., N. \tag{2.59}$$

The index j refers to the grid point and the number of grid points is given by N. The grid spacing Δx is given by $\Delta x = (x^{max} - x^{min})/(N-1)$.

The breakthrough in the numerical solution of the time-dependent Schrödinger equation was achieved when the fast Fourier transformation (FFT) technique was applied in [81, 67] for the evaluation of the kinetic energy part of the Hamiltonian. The essence of the method is the fact that the quantum mechanical momentum operators, nonlocal in the coordinate representation, are local in the momentum representation, where their action can be evaluated by a simple multiplication. This method was originally intended for determining the modes of optical wave guides, where the wave equations are similar to the Schrödinger equation. The underlying principles of this method will be outlined.

Let us first assume that the Hamilton operator $\hat{H}$ in Eq. [2.58] is explicitly time-independent. In this case its formal solution can be written

in the following form:

$$\psi(x,t) = e^{-i\hat{H}t}\psi(x,0) = e^{-i(\hat{T}+\hat{U})t}\psi(x,0), \tag{2.60}$$

where $\hat{T}$,$\hat{U}$ correspond to kinetic and potential energy operators. If we consider the evolution of the wave function during one time step Δt, the equation Eq. [2.60] then becomes:

$$\psi(x,t+\Delta t) = e^{-i(\hat{T}+\hat{U})\Delta t}\psi(x,t). \tag{2.61}$$

Since the potential and kinetic energy operators do not commute, we cannot rewrite the exponential of the sum of operators in Eq. [2.61] as a product of exponentials of each. Would such factorization to be performed, an error of the order of Δt^2 would be introduced in the energy. However, a certain arrangement of terms in the Hamilton operator allows to achieve higher accuracy. Let us consider the Baker-Campbell-Hausdorff theorem, applied to three operators $\hat{A}, \hat{B}, \hat{C}$:

$$\exp\left(\hat{A}\right)\exp\left(\hat{B}\right)\exp\left(\hat{C}\right) = \exp\Big(\hat{A}+\hat{B}+\hat{C}+ \frac{1}{2}\big([\hat{A},\hat{B}]+[\hat{B},\hat{C}]+[\hat{A},\hat{C}]\big)+...\Big). \tag{2.62}$$

Let us define the operators $\hat{A}, \hat{B}, \hat{C}$ as follows:

$$\hat{A} = \hat{C} = -i\frac{\hat{U}}{2}\Delta t, \hat{B} = -i\hat{T}\Delta t. \tag{2.63}$$

Substituting Eq. [2.63] into the equation Eq. [2.62] yields:

$$\exp\Big(-i\frac{\hat{U}}{2}\Delta t\Big)\exp\Big(-i\hat{T}\Delta t\Big)\exp\Big(-i\frac{\hat{U}}{2}\Delta t\Big) = \exp\Big(-i(\hat{T}+\hat{U})\Delta t+O(\Delta t^3)\Big). \tag{2.64}$$

Combining the equations Eq. [2.61] and Eq. [2.62], we obtain the split-operator propagator in the final form:

$$\psi(x,t+\Delta t) = e^{-i\frac{\hat{U}}{2}\Delta t}e^{-i\hat{T}\Delta t}e^{-i\frac{\hat{U}}{2}\Delta t}\psi(x,t) + O(\Delta t^3). \tag{2.65}$$

Thus, the split-operator method is accurate to the second term in the Δt.

Practical implementation of the split operator propagation requires the use of the FFT method, so that the actions of the operators will be evaluated in their respective local representations. Since the kinetic and potential energy operators are arguments of exponential functions, this procedure works only when the kinetic energy operator is diagonal in momentum space, for example, if it is given in Cartesian coordinates.

In order to derive the expression for the split-operator propagator an assumption was made, that the Hamilton operator is not explicitly time-dependent. If the Hamilton operator contains the time-dependent interaction part, this assumption does not hold. However, Kouri and coworkers

[68] have shown, that it is possible to derive an expression for the split-operator which accommodates the explicitly time-dependent Hamiltonians correctly, retaining the accuracy of the method. In this case the potential-type splitting has to be used, and the final expression for the propagator reads

$$\psi(x, t + \Delta t) = e^{-i\frac{\hat{U}(t+\Delta t)}{2}\Delta t} e^{-i\hat{T}\Delta t} e^{-i\frac{\hat{U}(t)}{2}\Delta t} \psi(x, t) + O(\Delta t^3). \qquad (2.66)$$

In the course of the propagation, an electron wavepacket may approach the end of the grid, on which it is defined, due to fast ionization. In this case further propagation will give rise to the reflection of the wave packet from the grid boundary. To prevent the unphysical behavior of the wave packet, one has to damp the wave function near the grid boundaries. A possible way to achieve this is to multiply the propagated wave function at each time step by a function which is equal to one in the grid regions where the dynamics takes place and rapidly goes to zero in the certain predefined region in the immediate vicinity of the boundary. This approach was suggested by Bisseling et al. [69] and is named as "absorbing boundary condition approach". Alternatively, one can implement an absorbing boundary condition by adding to the Hamiltonian an artificial purely imaginary potential-type term. Drawing parallels from optics, such a term is often called imaginary optical potential. With exponential-type propagators, like split-operator, these terms lead to efficient damping of the wave function in the regions, where this imaginary optical potential is defined. In contrast with the previous approach, this term has to be added to the potential only once before the propagation leading to considerable speedup in computation. We determine the initial wavefunction $\psi_0(x) = \psi(x, 0)$ and ions configuration $\{R_j\}$ for a given number of atoms N in the cluster using the Quantum Genetic Algorithm (see the Theory section [2.2]). We have checked that without external field the obtained 1D clusters are stable on the time interval of more than 1000 fs.